Imaging-Based Analysis of Circadian Reprogramming and Cellular Remodeling Induced by Time-Restricted Feeding in Aging and Neurodegeneration Models

Sachin Budhathoki , Palaniappan Sethu , Girish Melkani *

Posted Date: 18 May 2026

doi: 10.20944/preprints202605.1134.v1

Keywords: time-restricted feeding; cellular aging; neurodegeneration; circadian rhythm; cellular senescence; fluorescence microscopy; quantitative imaging; AC16 cardiomyocytes; metabolic reprogramming; cellular architecture; nutrient timing; in vitro models

 doi:10.20944/preprints202605.1134.v1

Article

Imaging-Based Analysis of Circadian Reprogramming and Cellular Remodeling Induced by Time-Restricted Feeding in Aging and Neurodegeneration Models

Sachin Budhathoki [1], Palaniappan Sethu [2,3] and Girish Melkani [1,4,*]

[1] Department of Pathology, Division of Molecular and Cellular Pathology, Heersink School of Medicine, The University of Alabama at Birmingham, AL 35294, USA

[2] Division of Cardiovascular Disease, Heersink School of Medicine, The University of Alabama at Birmingham, Birmingham, Alabama, USA

[3] Department of Biomedical Engineering, School of Engineering and School of Medicine, The University of Alabama at Birmingham, Birmingham, Alabama, USA

[4] UAB Nathan Shock Center, Birmingham, AL 35294, USA

* Correspondence: girishmelkani@uabmc.edu

Abstract

Time-restricted feeding (TRF) has emerged as a promising intervention to improve metabolic health and promote healthy aging, yet the cellular mechanisms underlying its effects remain incompletely understood. Here, we applied imaging-based and quantitative cellular analyses to investigate how TRF modulates aging-associated and neurodegeneration-related phenotypes in vitro. Human fibroblasts and AC16 cardiomyocytes were used as models of cellular aging, alongside fibroblast-based models of neurodegeneration. TRF was simulated through cyclic nutrient availability, and cellular responses were evaluated using microscopy-based assessment of cellular morphology, senescence-associated features, metabolic state, and circadian rhythm-associated gene expression dynamics. Imaging analyses demonstrated that TRF modulated key hallmarks of cellular senescence, including changes in cell morphology and intracellular organization, consistent with enhanced cellular resilience and altered metabolic adaptation. In AC16 cardiomyocytes, TRF influenced aging-associated cellular phenotypes, indicating that its effects extend beyond proliferative cell systems to cardiac-relevant models. In neurodegeneration-associated fibroblast models, TRF altered disease-related cellular signatures and stress-associated phenotypes, supporting a potential protective role in neurodegenerative conditions. Quantitative analyses further revealed significant TRF-induced changes in circadian rhythm characteristics across all models, including altered oscillatory amplitude, supporting a mechanistic link between nutrient timing and cellular timekeeping. Together, these findings demonstrate that TRF induces measurable changes in cellular architecture and circadian regulation associated with improved aging- and neurodegeneration-related phenotypes. This work highlights the utility of imaging-based approaches for investigating the spatiotemporal cellular effects of metabolic interventions and supports TRF as a potential therapeutic strategy for age-associated diseases.

Keywords: time-restricted feeding; cellular aging; neurodegeneration; circadian rhythm; cellular senescence; fluorescence microscopy; quantitative imaging; AC16 cardiomyocytes; metabolic reprogramming; cellular architecture; nutrient timing; in vitro models

 doi:10.20944/preprints202605.1134.v1

1. Introduction

Aging is a major risk factor for a wide range of chronic diseases, including cardiovascular and neurodegenerative disorders. A central feature of aging is the progressive disruption of homeostatic networks that coordinate energy metabolism, stress responses, and proteostasis [1,2]. At the cellular level, circadian rhythms regulate the temporal organization of metabolic and homeostatic processes [3]. Disruption of circadian timing is increasingly recognized as both a driver and a consequence of aging, as well as a contributing factor in neurodegenerative disease pathogenesis [4,5].

Nutrient-sensing pathways are tightly intertwined with circadian regulation, and interventions that modulate metabolic timing have shown promise in improving life- as well as health-span [6–9]. Time-restricted feeding (TRF), which limits nutrient intake to defined daily windows without necessarily reducing caloric intake, has been shown [10,11]to enhance metabolic efficiency, reduce inflammation, and extend lifespan [3,12,13]. While these systemic benefits are well documented, the extent to which TRF exerts direct, cell-autonomous effects particularly in human cellular models of aging and neurodegeneration remains less clear.

Zooming into these mechanisms requires reductionist systems that capture disease-relevant features while enabling precise control of nutrient timing. Cell-based systems provide a tractable framework to model core features of aging and disease under controlled conditions [14–16]. Human fibroblasts are widely used to study replicative and stress-induced aging and can capture aspects of disease-associated phenotypes, including those relevant to neurodegeneration [17–19]. In parallel, AC16 cardiomyocyte-like cells extend this approach to a metabolically active, cardiac-relevant setting in which circadian and metabolic coordination are critical [20]. Together, these systems enable direct interrogation of how temporally patterned nutrient availability modulates aging- and disease-associated molecular signatures and circadian dynamics across distinct cellular contexts.

In the present study, we investigated the effects of TRF-mimicking nutrient cycles in senescent fibroblasts, neurodegeneration-associated fibroblast models, and aging AC16 cardiomyocyte-like cells. Using quantitative immunofluorescence imaging and transcriptional profiling, we examined cellular and molecular markers associated with inflammation, oxidative stress, proteostasis, lipid metabolism, mitochondrial regulation, and circadian-associated homeostatic pathways. Imaging-based analyses were used to evaluate alterations in cellular morphology, intracellular organization, and senescence-associated phenotypes across experimental conditions. We further assessed how TRF-induced molecular and cellular changes relate to circadian rhythm characteristics across distinct cellular models. By integrating aging, neurodegeneration, metabolism, circadian biology, and imaging-based cellular analysis in controlled in vitro systems, this work provides insight into how temporal regulation of nutrient availability modulates cellular architecture, resilience, and disease-associated dysfunction.

2. Methods

2.1. Cell Culture, and Induction of Aging and Neurodegenerative

AC16 (Adult human ventricular cardiomyocyte/SV40-transformed hybrid) cells were obtained from ATCC (#CRL-3568) and maintained in Dulbecco's modified Eagle's medium (DMEM) supplemented with 10% fetal bovine serum (FBS) under standard culture conditions (37 °C, 5% CO_2). Human Dermal Fibroblasts, neonatal (HDFn) from ATCC (#PCS-201-010) was similarly cultured. Cells were used during the exponential growth phase for all experiments. To induce aging-associated cellular stress, doxorubicin (Sigma-Aldrich) was freshly prepared and added to the culture medium at a final concentration of 0.5 μM following established protocol [21]. The cells were exposed to doxorubicin for 24 h, after which the treatment medium was removed, and cells were washed twice with phosphate-buffered saline (PBS). Cells were then maintained in complete growth medium for an additional 48 h to allow recovery and stabilization. To model neurodegenerative-like cellular stress, HDFn were treated with okadaic acid (OA), a serine/threonine phosphatase (PP2A) inhibitor, with some modifications to established protocol [22]. OA was prepared as a concentrated 1 mM stock

 doi:10.20944/preprints202605.1134.v1

solution in DMSO and freshly diluted into PBS immediately prior to treatment. Cells were exposed to OA at a final concentration of 0.05 μM for 24 h. Following OA exposure, the cells were allowed to recover prior to downstream analyses.

2.2. Implementation of Time-Restricted Feeding (TRF) Regimen

To model TRF in vitro, we implemented a nutrient-timing regimen based on alternating periods of nutrient availability and deprivation. Prior to initiation of TRF, cells were subjected to serum-deprivation for 24 h for synchronizing circadian rhythms. Following synchronization, cells were returned to complete growth medium for 24 h to allow stabilization of rhythmic transcriptional activity. TRF was initiated thereafter and maintained for 2 consecutive days. Cells were exposed to complete growth medium for an 8-h feeding window (10:00–18:00), followed by a 16-h fasting period (18:00–10:00) in TRF medium. The TRF medium consisted of RPMI Medium 1640 (Gibco #11879-020) lacking glucose and serum. Media changes were performed daily at consistent times to preserve temporal fidelity. Control cells were cultured continuously in complete growth medium (ad libitum feeding, ALF).

2.3. Immunofluorescence Imaging and Quantitative Analysis

IF imaging and quantification was done with some modifications to our published method[23]. Briefly, cells were fixed with freshly prepared 4% paraformaldehyde (Electron Microscopy Sciences; 15,710), permeabilized as appropriate, and blocked in solution with 3% BSA and 10% Normal Donkey Serum. Then immunostaining was performed to assess global cellular state various stress markers. List of stains and antibodies are provided with supplementary information. Secondary fluorophores were selected based on their emission properties to minimize spectral overlap and ensure reliable signal discrimination. Imaging was performed on randomly selected, non-overlapping 15-20 fields from each sample using an Olympus BX-63 microscope fluorescence microscope and fluorescence intensity was quantified using CellSens software. Representative images were selected based on consistent staining quality and cell density.

2.4. RNA Isolation and RT-qPCR

Total RNA was isolated from cultured cell monolayers using the Quick-RNA™ Microprep Kit (Zymo Research; #R1050) according to the manufacturer's instructions. Briefly, cultured medium was removed, washed with PBS and cells were lysed directly on the culture surface using RNA Lysis Buffer. Cell lysates were collected by pipetting. Following ethanol addition, lysates were applied to Zymo-Spin™ IC columns. In-column DNase I digestion was performed to eliminate residual genomic DNA. Columns were sequentially washed using the supplied wash and prep buffers, and RNA was eluted in DNase/RNase-free water. Purified RNA was either used immediately for downstream applications or stored at −80 °C until use. RNA quantity and purity were assessed prior to cDNA synthesis. Reverse transcription was performed using equal amounts of RNA from each sample. Quantitative PCR was carried out using gene-specific primers for metabolic, mitochondrial, and stress-associated genes. Gene expression levels were normalized to a housekeeping gene 60s ribosomal protein (Rpl11) and expressed relative to the control condition using the ΔΔCt method.

2.5. Statistical Analysis

Statistical analyses were performed using GraphPad Prism (version 10). Statistical comparisons were performed using unpaired two-tailed t-tests with Welch's correction when variances were unequal. For time-series RT-qPCR experiments, comparisons across time points and feeding conditions were analyzed using two-way analysis of variance (ANOVA) with repeated measures. When significant main or interaction effects were detected, Šídák's multiple-comparison test was applied for post hoc analysis. Data are presented as mean ± SEM. Statistical significance was defined

 doi:10.20944/preprints202605.1134.v1

as $p < 0.05$ (*), $p < 0.01$ (**) and $p < 0.001$ (***). Exact sample sizes, statistical tests, and post hoc analyses used for each experiment are specified in the corresponding figure legends.

3. Results

3.1. TRF Attenuates Senescence and Inflammation in Aging Fibroblasts

To assess the impact of TRF on cellular aging, we examined senescence- and stress-associated markers in fibroblasts. TRF decreased CASP8 (Figure 1 C1, D), NF-κB2 (Figure 1 C2, E), and CDKN levels (Figure 1 C4, G), indicating attenuation of apoptosis-associated signaling, inflammatory activation, and senescence-associated pathways. In contrast to these reductions, ATP1A1 expression was increased under TRF conditions (Figure 1 C3, F), suggesting altered cellular energetic state. While Actinin and Collagen IV levels remained largely comparable between conditions (SI 1 A2, A3, C, D), TRF increased p62 accumulation (SI 1 A), indicating modulation of proteostatic pathways distinct from the reductions observed in inflammatory markers. RT–qPCR analysis further supported broad metabolic remodeling in TRF-treated fibroblasts. TRF increased TFAM (Figure 1 I), PPARGC1A (Figure 1 J), PRKAA (Figure 1 K), PNPLA2 (Figure 1 M), SIRT1 (Figure 1 L), and ATP2A2 expression (Figure 1 N), while IL6 (Figure 1 O) and TGFB1 (Figure 1 H) were decreased. Together, these findings indicate that TRF suppresses senescence-associated stress signaling while enhancing transcriptional programs linked to mitochondrial and metabolic regulation. Consistent with these observations, modulation of SIRT1 and PRKAA further suggested engagement of circadian-associated metabolic pathways in aging fibroblasts.

3.2. TRF Reduces Proteotoxic Stress and Stress-Associated Signaling in Neurodegeneration-Like Fibroblast Model

To model neurodegeneration-associated stress, fibroblasts were treated with okadaic acid. Similar to the aging fibroblast model, TRF reduced CASP8 (Figure 2 C1, D), NF-κB2 (Figure 2 C2, E), and CDKN expression (Figure 2 C4, G), indicating suppression of apoptosis-, inflammation-, and senescence-associated signaling under proteotoxic stress conditions. In contrast to the increased ATP1A1 observed in aging fibroblasts, ATP1A1 expression was reduced in okadaic acid–treated cells under TRF conditions (Figure 2 C3, F), highlighting a context-dependent metabolic response. TRF also decreased p62 levels and lipid droplet accumulation, supporting altered proteostatic and lipid-handling pathways during neurodegenerative-like stress. Actinin levels remained comparable between conditions (SI 2 A2, C), whereas Collagen IV deposition was decreased (SI 2 A3, D).

At the transcriptional level, TRF increased TFAM (Figure 2 I), PRKAA (Figure 2 K), PNPLA2 (Figure 2 M), and ATP2A2 expression (Figure 2 N), while PPARGC1A showed an increasing trend (Figure 2 J). In contrast to the aging fibroblast model, SIRT1 expression demonstrated a decreasing trend under TRF conditions (Figure 2 L), despite a concurrent decreasing trend in IL6 expression (Figure 2 O), suggesting that proteotoxic stress may differentially influence metabolic and circadian-associated regulatory pathways. Together, these findings indicate that although TRF consistently attenuates stress-associated signaling across fibroblast models, the direction and magnitude of metabolic responses differ depending on the underlying cellular stress context.

3.3. TRF Improves Metabolic and Stress-Associated Signatures in Aging AC16 Cardiomyocyte-Like Cells

To determine whether TRF-associated effects extend beyond fibroblasts, we examined AC16 cardiomyocyte-like cells subjected to aging-associated stress. Similar to both fibroblast models, TRF decreased CASP8 (Figure 3 C1, D), NF-κB2 (Figure 3 C2, E), and CDKN expression (Figure 3 C4, G), supporting a conserved reduction in apoptosis-, inflammation-, and senescence-associated signaling across cell types. However, unlike aging fibroblasts, ATP1A1 expression showed a decreasing trend in AC16 cells under TRF conditions (Figure 3 C3, F), indicating cell-type-specific metabolic adaptation. Actinin levels remained comparable between conditions (SI 3 A2, C), while Collagen IV exhibited a decreasing trend (SI 3 A3, D).

 doi:10.20944/preprints202605.1134.v1

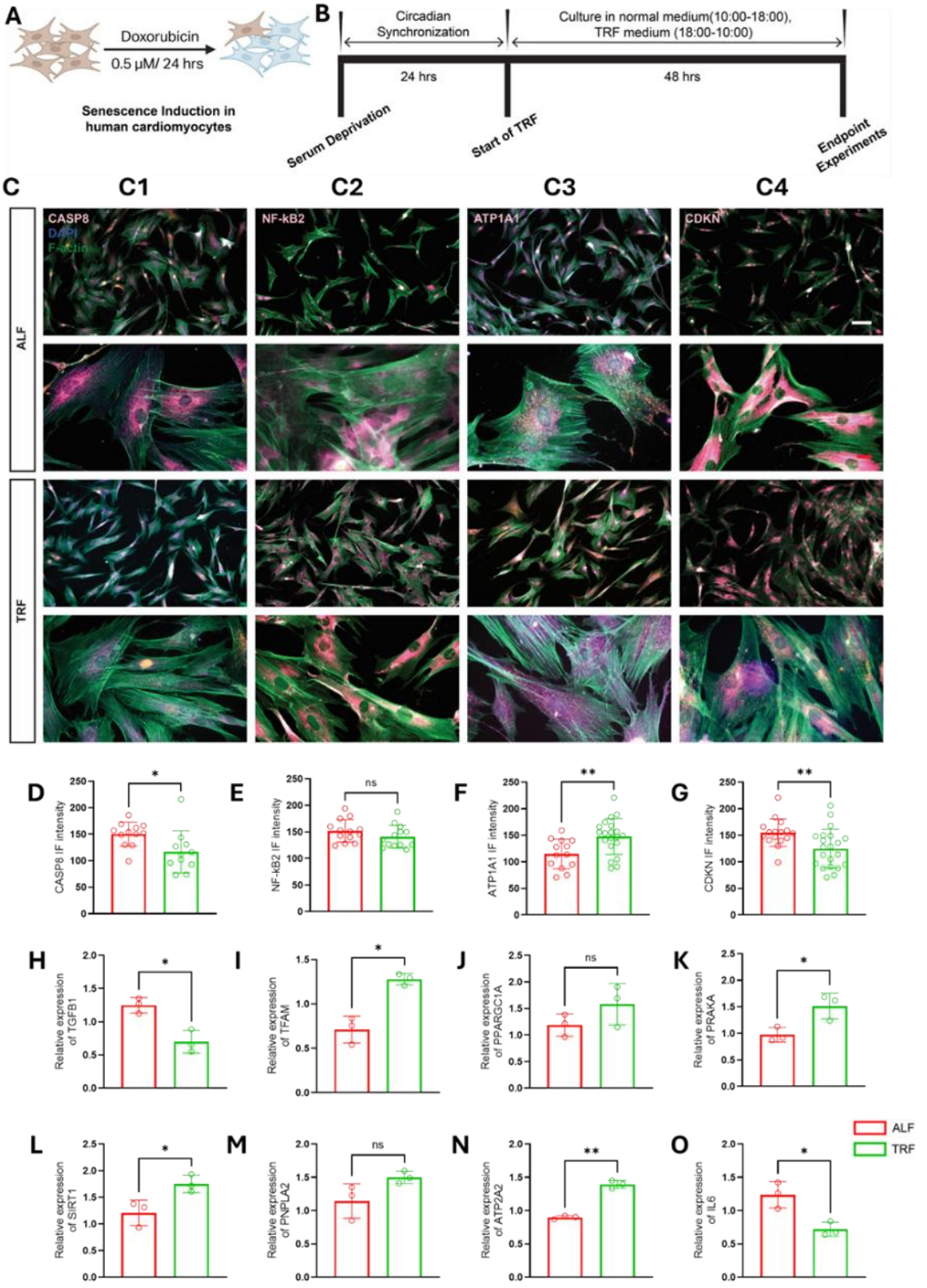

Figure 1. TRF attenuates aging-associated stress signaling and modulates metabolic gene expression in senescent human fibroblasts. (A) Schematic illustrating induction of aging-associated cellular stress by doxorubicin treatment (0.5 μM, 24 h) (B) Experimental timeline showing TRF Regimen. Circadian synchronization by serum deprivation (24 h) preceded initiation of TRF with culture under alternating feeding (10:00–18:00) and fasting (18:00–10:00) conditions for 48 h before endpoint analyses. (C) Representative immunofluorescence images of senescent human dermal fibroblasts cultured under ad libitum feeding (ALF) or TRF conditions. Cells were stained for CASP8 (C1), NF-κB2 (C2), ATP1A1 (C3), and CDKN1A (C4), with F-actin and DAPI used to visualize

 doi:10.20944/preprints202605.1134.v1

cytoskeletal organization and nuclei, respectively. Scale bars: White-100 μm, Red-20 μm. (D–G) Quantification of immunofluorescence intensity as arbitrary units for CASP8 (D), NF-κB2 (E), ATP1A1 (F), and CDKN1A (G) under ALF and TRF conditions. Data are presented as mean ± SEM (n = 15-20 images). (H–O) RT-qPCR analysis of stress and metabolism-associated gene expression in senescent fibroblasts cultured under ALF or TRF conditions. Expression levels of TGFB1 (H), TFAM (I), PPARGC1A (J), PRKAA1 (K), SIRT1 (L), PNPLA2 (M), ATP2A2 (N), and IL6 (O) are shown relative to ALF controls and normalized to the housekeeping gene RPL11. Data means SEM (n = 3 biological replicates). Statistical comparisons were performed using unpaired two-tailed t-tests with Welch's correction (*p < 0.05, **p < 0.01; ns, not significant).

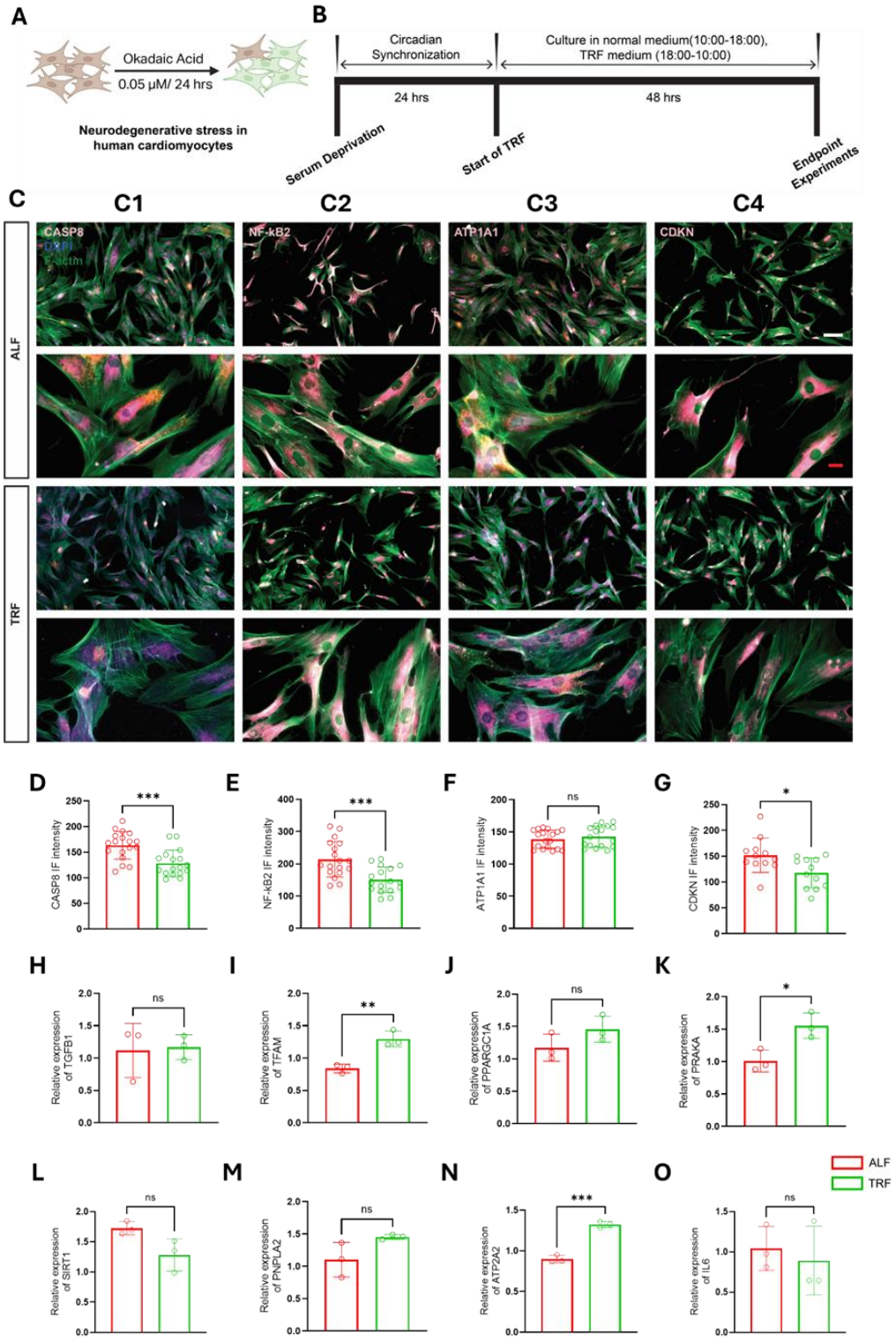

 doi:10.20944/preprints202605.1134.v1

Figure 2. TRF attenuates stress-associated signaling and modulates metabolic gene expression in a neurodegenerative-like fibroblast model. (A) Schematic illustrating induction of neurodegenerative-like cellular stress in neonatal human dermal fibroblasts (HDFn) by okadaic acid treatment (0.05 μM, 24 h). (B) Experimental timeline showing the TRF regimen. Circadian synchronization by serum deprivation (24 h) preceded initiation of TRF, with culture under alternating feeding (10:00–18:00) and fasting (18:00–10:00) conditions for 48 h prior to endpoint analyses. (C) Representative immunofluorescence images of okadaic acid–treated fibroblasts cultured under ad libitum feeding (ALF) or TRF conditions. Cells were stained for CASP8 (C1), NF-κB2 (C2), ATP1A1 (C3), and CDKN1A (C4), with F-actin and DAPI used to visualize cytoskeletal organization and nuclei, respectively. Scale bars: white-100 μm; red-20 μm. (D–G) Quantification of immunofluorescence intensity as arbitrary units for CASP8 (D), NF-κB2 (E), ATP1A1 (F), and CDKN1A (G) under ALF and TRF conditions. Data are presented as mean ± SEM (n = 15–20 images). (H–O) RT-qPCR analysis of stress and metabolism-associated gene expression in okadaic acid–treated fibroblasts cultured under ALF or TRF conditions. Expression levels of TGFB1 (H), TFAM (I), PPARGC1A (J), PRKAA1 (K), SIRT1 (L), PNPLA2 (M), ATP2A2 (N), and IL6 (O) are shown relative to ALF controls and normalized to the housekeeping gene RPL11. Data means SEM (n = 3 biological replicates). Statistical comparisons were performed using unpaired two-tailed t-tests with Welch's correction ($p < 0.05$, $p < 0.01$, $p < 0.001$; ns, not significant).

RT–qPCR analysis revealed increased TFAM (Figure 3 I) and PPARGC1A expression (Figure 3 J), suggesting enhanced mitochondrial and metabolic regulation in TRF-treated AC16 cells. PNPLA2 and SIRT1 also demonstrated increasing trends (Figure 3 M, L), whereas PRKAA showed a decreasing trend (Figure 3 K). In contrast to the fibroblast models, IL6 expression increased under TRF conditions (Figure 3 O), while TGFB1 expression remained largely comparable between groups (Figure 3 H), indicating that inflammatory and metabolic transcriptional responses to TRF differ between fibroblast and cardiomyocyte-like systems. Together, these findings suggest that although TRF engages conserved stress-associated pathways across models, downstream metabolic and inflammatory responses remain context.

3.4. TRF Induces Context-Dependent Modulation of Circadian-Associated Gene Expression Across Cellular Models

Given the established relationship between nutrient timing and circadian regulation, we next examined temporal expression patterns of core circadian genes across the different cellular models. Time-series RT–qPCR analysis of BMAL1, CLOCK, and PER2 revealed that TRF altered circadian-associated transcriptional dynamics in a model-dependent manner rather than producing uniform changes across all systems.

In doxorubicin-induced senescent fibroblasts, TRF was associated with greater temporal variation in PER2 expression (Figure 4 C), including a more pronounced intermediate peak relative to ALF conditions, while BMAL1 and CLOCK maintained oscillatory expression profiles with altered amplitudes (Figure 4 A, B). In contrast, okadaic acid–treated fibroblasts exhibited comparatively dampened temporal expression patterns, particularly for PER2 (Figure 4 F), suggesting that proteotoxic stress alters circadian responsiveness under TRF conditions. AC16 cardiomyocyte-like cells displayed more modest TRF-associated effects, with BMAL1, CLOCK, and PER2 largely maintaining oscillatory trends across time points (Figure 4 G–I). Together, these findings indicate that TRF engages circadian-associated transcriptional programs across distinct cellular contexts, although the magnitude and direction of these responses vary depending on cell type and stress condition. The parallel modulation of circadian-associated genes alongside metabolic and stress-response pathways further supports an interaction between temporal nutrient availability and intrinsic cellular regulatory networks.

 doi:10.20944/preprints202605.1134.v1

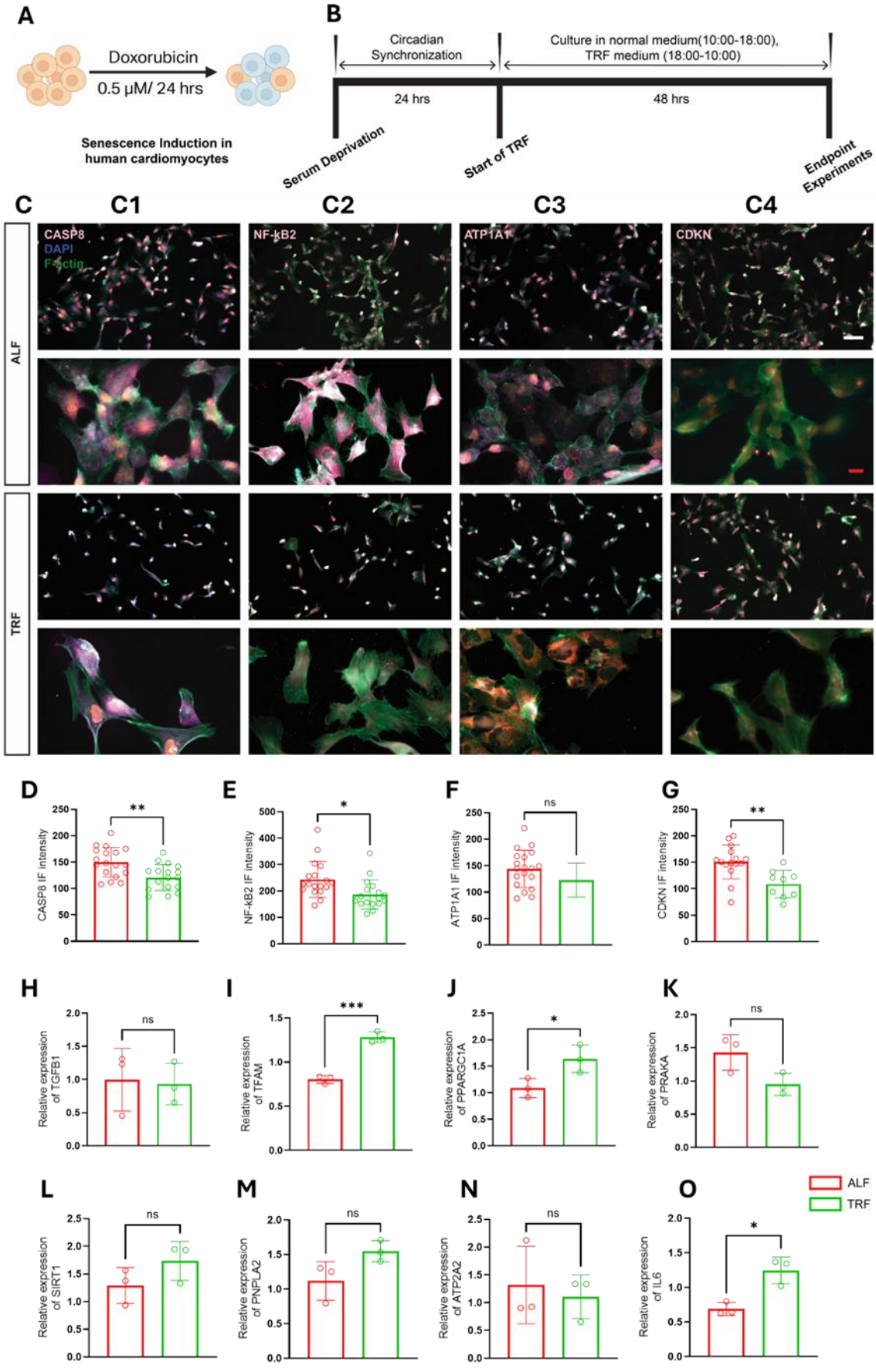

Figure 3. TRF attenuates aging-associated stress signaling and modulates metabolic gene expression in senescent AC16 cardiomyocyte-like cells. (A) Schematic illustrating induction of aging-associated cellular stress in AC16

 doi:10.20944/preprints202605.1134.v1

cardiomyocyte-like cells by doxorubicin treatment (0.5 μM, 24 h). (B) Experimental timeline showing the TRF regimen. Circadian synchronization by serum deprivation (24 h) preceded initiation of TRF, with culture under alternating feeding (10:00–18:00) and fasting (18:00–10:00) conditions for 48 h prior to endpoint analyses. (C) Representative immunofluorescence images of doxorubicin-treated AC16 cells cultured under ad libitum feeding (ALF) or TRF conditions. Cells were stained for CASP8 (C1), NF-κB2 (C2), ATP1A1 (C3), and CDKN1A (C4), with F-actin and DAPI used to visualize cytoskeletal organization and nuclei, respectively. Scale bars: white-100 μm; red-20 μm. (D–G) Quantification of immunofluorescence intensity as arbitrary units for CASP8 (D), NF-κB2 (E), ATP1A1 (F), and CDKN1A (G) under ALF and TRF conditions. Data are presented as mean ± SEM (n = 15–20 images). (H–O) RT-qPCR analysis of stress and metabolism-associated gene expression in doxorubicin-treated AC16 cells cultured under ALF or TRF conditions. Expression levels of TGFB1 (H), TFAM (I), PPARGC1A (J), PRKAA1 (K), SIRT1 (L), PNPLA2 (M), ATP2A2 (N), and IL6 (O) are shown relative to ALF controls and normalized to the housekeeping gene RPL11. Data means SEM (n = 3 biological replicates). Statistical comparisons were made using unpaired two-tailed t-tests with Welch's correction ($p < 0.05$, $p < 0.01$; ns, not significant).

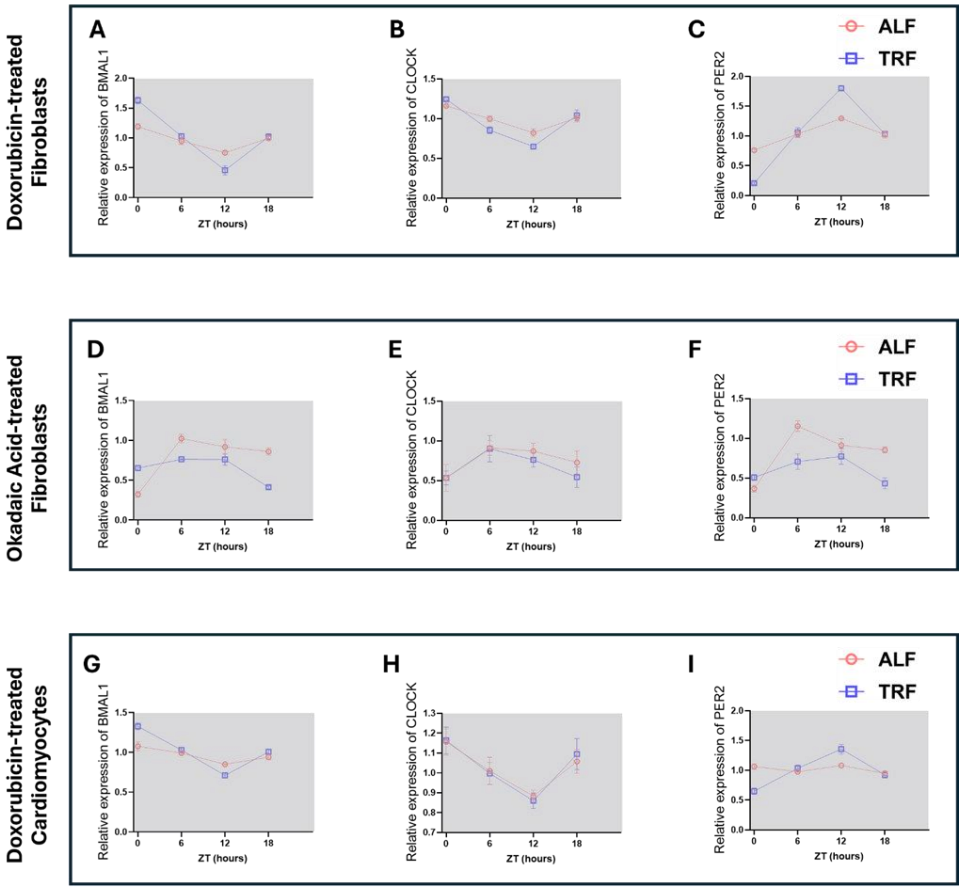

Figure 4. Time-restricted feeding induces context-dependent modulation of circadian-associated gene expression across cellular stress models. (A–C) Time-series RT-qPCR analysis of BMAL1 (A), CLOCK (B), and PER2 (C) expression in doxorubicin-treated senescent human dermal fibroblasts cultured under ad libitum feeding (ALF) or time-restricted feeding (TRF) conditions. Gene expression was measured at indicated Zeitgeber times (ZT; hours). (D–F) Time-series RT-qPCR analysis of BMAL1 (D), CLOCK (E), and PER2 (F) expression in okadaic acid–treated fibroblasts under ALF or TRF conditions. (G–I) Time-series RT-qPCR analysis of BMAL1 (G), CLOCK (H), and PER2 (I) expression in doxorubicin-treated AC16 cardiomyocyte-like cells under ALF or TRF conditions. For all panels, expression levels are shown relative to the housekeeping gene RPL11. Data are presented as mean ± SEM (n = 3 biological replicates per time point). Statistical comparisons across feeding conditions and time points were performed using two-way repeated-measures ANOVA, followed by Šídák's multiple-comparison test.

 doi:10.20944/preprints202605.1134.v1

4. Discussion

This study demonstrates that time-restricted feeding (TRF) produces a coordinated but context-dependent cellular response across multiple models of aging and stress. Despite differences in cellular identity and insult type, TRF consistently attenuated stress-associated phenotypes in doxorubicin-induced senescent fibroblasts, okadaic acid–treated fibroblasts, and aging-associated AC16 cardiomyocyte-like cells. In aging fibroblasts, TRF reduced CASP8, NF-κB2, and CDKN expression (Figure 1 C1, D; C2, E; C4, G), accompanied by increased ATP1A1 levels (Figure 1 C3, F) and transcriptional upregulation of TFAM, PPARGC1A, PRKAA, and SIRT1 (Figure 1 I–L). A similar reduction in inflammatory and senescence-associated signaling was observed in the okadaic acid-treated neurodegenerative model, where TRF decreased CASP8, NF-κB2, and CDKN expression (Figure 2 C1, D; C2, E; C4, G), alongside reduced Collagen IV deposition (SI 2 A3, D) and altered metabolic gene expression. In AC16 cells, TRF suppressed CASP8, NF-κB2, and CDKN (Figure 3 C1, D; C2, E; C4, G), indicating that attenuation of stress-associated signaling represents a conserved response across both fibroblast and cardiomyocyte-like systems.

Although these convergent phenotypes point toward shared TRF-responsive pathways, important differences between models suggest that the downstream cellular response is shaped by both stress context and cell identity. In aging fibroblasts, TRF was associated with increased ATP1A1 expression (Figure 1 C3, F), whereas ATP1A1 decreased in both okadaic acid–treated fibroblasts and AC16 cells (Figure 2 C3, F; Figure 3 C3, F), indicating that energetic adaptation under TRF differs between chronic senescence and proteotoxic or cardiac stress conditions. Similarly, p62 accumulation increased in aging fibroblasts (SI 1 A) but decreased in the okadaic acid model, suggesting distinct proteostatic demands between senescence-associated remodeling and acute proteotoxic injury[24,25]. Transcriptional responses also diverged across systems. While fibroblast aging showed coordinated increases in TFAM, PPARGC1A, PRKAA, and SIRT1 (Figure 1 I–L), the okadaic acid model displayed a decreasing trend in SIRT1 despite increased PRKAA and TFAM expression (Figure 2 I–L). In AC16 cells, PRKAA exhibited a decreasing trend while IL6 expression increased under TRF conditions (Figure 3 K, O), contrasting with the anti-inflammatory transcriptional profile observed in fibroblasts.

An important observation emerging from this study is that not all markers responded equivalently to TRF, and these nonuniform responses likely reflect underlying biological variables. Structural markers such as Actinin remained largely comparable across conditions in both fibroblast and AC16 models (SI 1 A2, C; SI 2 A2, C; SI 3 A2, C), despite substantial changes in inflammatory and metabolic readouts. This suggests that TRF-induced adaptation preferentially targets dynamic stress-responsive pathways before inducing overt structural remodeling[26]. Similarly, Collagen IV exhibited more modest and context-dependent changes relative to inflammatory markers, with clearer reductions observed in the okadaic acid model (SI 2 A3, D) than in aging fibroblasts (SI 1 A3, D). Given the stability and slow turnover of extracellular matrix-associated proteins, these findings may reflect temporal differences in pathway responsiveness rather than absence of biological effect. The divergence in p62 behavior between fibroblast models also emphasizes the importance of context in interpreting proteostatic markers, as accumulation of p62 can reflect either impaired degradation or adaptive remodeling depending on the underlying cellular state.

The circadian analyses provide a framework through which these context-dependent TRF responses can be interpreted. Time-series RT–qPCR analysis of BMAL1, CLOCK, and PER2 revealed that nutrient timing altered circadian-associated transcriptional dynamics across all three models, although the magnitude and pattern of these changes differed substantially by condition (Figure 4 A–I). In doxorubicin-induced senescent fibroblasts, TRF enhanced temporal variation in PER2 expression (Figure 4 C) while maintaining oscillatory BMAL1 and CLOCK profiles with altered amplitudes (Figure 4 A, B). In contrast, okadaic acid–treated fibroblasts displayed comparatively dampened circadian-associated expression patterns, particularly for PER2 (Figure 4 F), suggesting that proteotoxic stress may impair circadian responsiveness under nutrient-restricted conditions[27]. AC16 cardiomyocyte-like cells showed comparatively stable oscillatory trends across BMAL1,

 doi:10.20944/preprints202605.1134.v1

CLOCK, and PER2 expression (Figure 4 G–I), indicating that circadian-associated regulation may be preserved differently in cardiac-like cells under stress.

These observations are particularly relevant given the established integration between circadian regulation, metabolic signaling, and cellular stress responses. The recurrent modulation of SIRT1 and PRKAA across multiple datasets (Figure 1 K, L; Figure 2 K, L; Figure 3 K, L) supports the possibility that TRF-associated metabolic adaptation occurs in parallel with changes in circadian-associated regulatory networks[28]. Importantly, the circadian data in this study should not be interpreted as evidence of restored rhythmicity or clock function, as functional oscillatory output was not directly assessed. Rather, the findings suggest that temporal nutrient restriction alters the transcriptional organization of circadian-associated pathways in a manner that parallels broader changes in stress and metabolic state. This interpretation is consistent with the observation that models exhibiting the strongest stress-associated phenotypes, particularly the okadaic acid condition, also demonstrated the greatest disruption in circadian-associated expression patterns.

Several pathways demonstrated strong agreement across datasets, particularly inflammatory signaling and mitochondrial-associated regulation. Reductions in NF-κB2 protein expression were accompanied by decreases in IL6 transcription in fibroblast models (Figure 1 C2, E, O; Figure 2 C2, E, O), while increased TFAM and PPARGC1A expression paralleled shifts in ATP1A1 and lipid-associated readouts. However, other pathways showed weaker alignment between transcriptional and protein-level measurements, particularly extracellular matrix-associated and proteostatic markers. These differences likely reflect temporal separation between transcriptional activation and protein turnover, as well as post-transcriptional regulation that cannot be captured through endpoint RT–qPCR alone[29]. The combined use of imaging-based phenotyping and transcriptional profiling therefore provides a more comprehensive representation of TRF-associated adaptation than either modality independently.

5. Conclusions

This study demonstrates that time-restricted feeding (TRF) modulates aging- and stress-associated phenotypes across multiple in vitro cellular models, including senescent fibroblasts, neurodegeneration-like fibroblasts, and aging AC16 cardiomyocyte-like cells. Despite differences in cell type and stress paradigm, TRF consistently attenuated inflammatory and senescence-associated signaling while altering metabolic and mitochondrial regulatory pathways. These shared responses were accompanied by context-dependent differences in proteostatic and metabolic adaptation, indicating that the cellular effects of TRF are shaped by both intrinsic cell identity and the nature of the underlying stress state. Importantly, integration of time-series circadian analyses revealed that TRF influences circadian-associated transcriptional dynamics across all models, linking nutrient timing with broader cellular regulatory programs. Although the magnitude and direction of circadian-associated changes varied between conditions, the parallel modulation of metabolic regulators such as SIRT1 and PRKAA suggests that circadian-associated pathways may represent a common framework through which TRF coordinates cellular adaptation. These findings support a role for temporal regulation of nutrient availability in shaping cellular stress responses across aging- and disease-associated states and provide a framework for future studies examining how metabolic timing influences cell-intrinsic resilience.

6. Limitation and Future Directions

Several limitations should be considered when interpreting these findings. Although, our TRF duration is influenced by comparable to published works[30–33], it is a relatively short regimen. Longer TRF durations or optimization of feeding–fasting intervals may produce more pronounced or mechanistically distinct effects, particularly for pathways related to extracellular remodeling, proteostasis, and circadian regulation that may require extended temporal adaptation[34]. The experimental systems used in this study also present inherent biological limitations. Fibroblasts

 doi:10.20944/preprints202605.1134.v1

provide a robust and tractable system for modeling cellular stress responses, senescence-associated phenotypes, and disease-relevant metabolic alterations, making them well suited for interrogating conserved cellular adaptation pathways under defined experimental conditions. However, fibroblasts do not fully recapitulate the specialized physiology of neurons or other disease-relevant cell types involved in neurodegeneration. Consequently, such findings should be interpreted as modeling proteotoxic and stress-associated cellular features rather than neuronal pathology itself.

Future studies incorporating three-dimensional culture systems, engineered tissues, or organoid models could improve physiological relevance by better preserving cell–cell interactions, spatial organization, and nutrient gradients. Such systems may also provide a more suitable framework for studying long-term TRF-associated adaptation and circadian regulation without risking over confluence likely in monolayer culture. In vitro studies like this would also benefit from the incorporation of human induced pluripotent stem cell (hiPSC)-derived systems, particularly patient-derived cells differentiated into neuronal or cardiac lineages. Compared with fibroblasts, hiPSC-derived neuronal models would provide greater disease relevance for neurodegeneration-associated studies while preserving patient-specific genetic and epigenetic backgrounds. Integration of TRF paradigms into these systems may help determine whether the conserved stress- and metabolism-associated responses observed in fibroblasts extend to more physiologically specialized and clinically relevant cellular contexts.

Finally, although the present study identified modulation of circadian-associated genes across multiple models, the analysis was limited to transcriptional measurements of selected clock-associated markers. Future studies incorporating higher-resolution temporal sampling, real-time circadian reporters, metabolic flux analysis, and functional mitochondrial assays will be important to define the mechanistic relationship between nutrient timing, circadian regulation, and cellular resilience.

References

1. Hartl, F.U., *Cellular Homeostasis and Aging.* Annual Review of Biochemistry, 2016. **85**(Volume 85, 2016): p. 1-4.
2. Hipp, M.S., P. Kasturi, and F.U. Hartl, *The proteostasis network and its decline in ageing.* Nature Reviews Molecular Cell Biology, 2019. **20**(7): p. 421-435.
3. de Assis, L.V.M. and H. Oster, *The circadian clock and metabolic homeostasis: entangled networks.* Cellular and Molecular Life Sciences, 2021. **78**(10): p. 4563-4587.
4. Verma, A.K., S. Singh, and S.I. Rizvi, *Aging, circadian disruption and neurodegeneration: Interesting interplay.* Experimental Gerontology, 2023. **172**: p. 112076.
5. Maidh, A., et al., Circadian disruption as a driver and target in neurodegenerative diseases: from molecular mechanisms to chronotherapeutic strategies. Metabolic Brain Disease, 2026. **41**(1): p. 62.
6. Melkani, G.C. and S. Panda, *Time-restricted feeding for prevention and treatment of cardiometabolic disorders.* The Journal of physiology, 2017. **595**(12): p. 3691-3700.
7. Roth, J.R., et al., Circadian-mediated regulation of cardiometabolic disorders and aging with time-restricted feeding. Obesity (Silver Spring), 2023. **31 Suppl 1**(Suppl 1): p. 40-49.
8. Zhong, D., et al., Interplay between aging and metabolic diseases: from molecular mechanisms to therapeutic horizons. Medical Review, 2025. **5**(6): p. 477-489.
9. Anton, S.D., et al., Flipping the Metabolic Switch: Understanding and Applying the Health Benefits of Fasting. Obesity (Silver Spring), 2018. **26**(2): p. 254-268.
10. Manoogian, E.N.C., et al., Time-restricted Eating for the Prevention and Management of Metabolic Diseases. Endocr Rev, 2022. **43**(2): p. 405-436.
11. Acosta-Rodríguez, V., et al., Circadian alignment of early onset caloric restriction promotes longevity in male C57BL/6J mice. Science, 2022. **376**(6598): p. 1192-1202.
12. Guo, Y., C. Livelo, and G.C. Melkani, Time-restricted feeding regulates lipid metabolism under metabolic challenges. BioEssays, 2023. **45**(12): p. 2300157.

 doi:10.20944/preprints202605.1134.v1

13. Chaix, A., et al., *Time-restricted eating to prevent and manage chronic metabolic diseases.* Annual review of nutrition, 2019. **39**(1): p. 291-315.
14. Kim, B., et al., *Cellular Models of Aging and Senescence.* Cells, 2025. **14**(16): p. 1278.
15. Lutolf, M.P., et al., In vitro human cell-based models: What can they do and what are their limitations? Cell, 2024. **187**(17): p. 4439-4443.
16. Fischer, D.S., et al., Adapting systems biology to address the complexity of human disease in the single-cell era. Nature Reviews Genetics, 2025. **26**(8): p. 514-531.
17. Olesen, M.A., F. Villavicencio-Tejo, and R.A. Quintanilla, *The use of fibroblasts as a valuable strategy for studying mitochondrial impairment in neurological disorders.* Translational Neurodegeneration, 2022. **11**(1): p. 36.
18. Teves, J.M.Y., et al., Parkinson's Disease Skin Fibroblasts Display Signature Alterations in Growth, Redox Homeostasis, Mitochondrial Function, and Autophagy. Frontiers in Neuroscience, 2018. **Volume 11—2017**.
19. Auburger, G., et al., *Primary skin fibroblasts as a model of Parkinson's disease.* Mol Neurobiol, 2012. **46**(1): p. 20-7.
20. Alan, L., et al., Mitochondrial metabolism and hypoxic signaling in differentiated human cardiomyocyte AC16 cell line. Am J Physiol Cell Physiol, 2025. **328**(5): p. C1571-c1585.
21. Budhathoki, S., et al., Engineered Aging Cardiac Tissue Chip Model for Studying Cardiovascular Disease. Cells Tissues Organs, 2021. **211**(3): p. 348-359.
22. Zhang, Z. and J.W. Simpkins, Okadaic acid induces tau phosphorylation in SH-SY5Y cells in an estrogen-preventable manner. Brain Res, 2010. **1345**: p. 176-81.
23. Watson, J.C., S. Budhathoki, and G.C. Melkani, *Novel And Efficient Method for Drosophila Heart Fluorescence Staining with Cryosectioning.* Journal of visualized experiments : JoVE, 2025. **217**.
24. Sabath, N., et al., *Cellular proteostasis decline in human senescence.* Proceedings of the National Academy of Sciences, 2020. **117**(50): p. 31902-31913.
25. Watts, T., et al., Declining intracellular proteostasis capacity drives misfolded protein secretion in senescent human cells. bioRxiv, 2025: p. 2025.09.07.674107.
26. Yan, L., B.M. Rust, and D.G. Palmer, Time-restricted feeding restores metabolic flexibility in adult mice with excess adiposity. Frontiers in Nutrition, 2024. **Volume 11—2024**.
27. Aoyama, S., Y. Nakahata, and K. Shinohara, *Chrono-Nutrition Has Potential in Preventing Age-Related Muscle Loss and Dysfunction.* Frontiers in Neuroscience, 2021. **Volume 15—2021**.
28. Deota, S., et al., Diurnal transcriptome landscape of a multi-tissue response to time-restricted feeding in mammals. Cell Metab, 2023. **35**(1): p. 150-165.e4.
29. Martin, E.W. and M.-H. Sung, Challenges of Decoding Transcription Factor Dynamics in Terms of Gene Regulation. Cells, 2018. **7**(9): p. 132.
30. Shi, D., et al., Six-hour time-restricted feeding inhibits lung cancer progression and reshapes circadian metabolism. BMC Med, 2023. **21**(1): p. 417.
31. Zhang, K., et al., Time-restricted feeding downregulates cholesterol biosynthesis program via RORγ-mediated chromatin modification in porcine liver organoids. J Anim Sci Biotechnol, 2020. **11**(1): p. 106.
32. Galigniana, N.M., et al., Transcriptional and Metabolic Changes Following Repeated Fasting and Refeeding of Adipose Stem Cells Highlight Adipose Tissue Resilience. Nutrients, 2024. **16**(24): p. 4310.
33. Yang, J., et al., Intermittent starvation promotes maturation of human embryonic stem cell-derived cardiomyocytes. Frontiers in Cell and Developmental Biology, 2021. **9**: p. 687769.
34. Dudek, M., J. Swift, and Q.-J. Meng, *The circadian clock and extracellular matrix homeostasis in aging and age-related diseases.* American Journal of Physiology-Cell Physiology, 2023. **325**(1): p. C52-C59.